Micro electric-field sensor based on converse piezoelectric effect

Mingyong Xin[1], Changbao Xu[1], Jianyang Zhu[1], Peng Li[2], Bing Tian[2], Zhong Liu[2], Zhifei Han[2]*

[1] *Guizhou Electric Power Research Institute, Guiyang, China*
[2] *Digital Grid Research Institute, China Southern Power Grid, Guangzhou, China*
**386872610@qq.com*

Keywords: Electric-field measurement, micro-fabrication, piezoelectric film, piezoresistive effect

Abstract

The measurement of electric field has important value for power grid information measurement, equipment fault diagnosis, meteorological monitoring, etc. Meanwhile, electric field measurement can also be used for voltage measurement. Traditional electric field measurement methods, such as field mills, are bulky and costly, and will cause electric field distortion. Micro electric field sensors have advantages of low cost, small size and easy mass production. At the same time, miniature sensors can reduce electric field distortion. Therefore, micro electric field sensors can be used in the applications such as large-scale sensing arrays, internal measurement of equipment, etc. In this paper, we proposed a novel micro electric field sensor based on PVDF film and piezoresistive effect. The proposed sensor has the advantages of wide frequency bandwidth and wide measuring range. Through micro-fabrication, the sensor can be mass produced.

1 Introduction

Ubiquitous Power Internet of Things is realized by setting up an information network corresponding to the energy network [1-2]. Using different types of sensors for measurement, the operating status of the power grid and equipment can be monitored in real time. Through the processing of a large amount of data, the status monitoring of the system and the fault diagnosis of the equipment can be realized. In the Ubiquitous Power Internet of Things, sensor nodes composed of advanced sensors are an important component.

Among all physical quantities, electric field is of great importance. On the one hand, the voltage can be measured by measuring the electric field at multiple points through the inversion algorithm [3]. Therefore, the electric field measurement can realize the non-contact measurement of voltage, avoiding the cost due to insulation. By measuring voltage, power grid monitoring and early warning and status perception can be realized [4-7]. On the other hand, electric field measurement also has important applications in other scenarios. Electric field measurement can realize electromagnetic environment monitoring, internal fault diagnosis of equipment, and warning of workers near electricity [8]. Electric field measurement is also widely used in lightning warning, aviation launch, petrochemical and other fields [9-10].

At present, the most widely studied micro electric field sensor is optical sensor based on electro-optic effect [11-14]. The refractive index of the electro-optic crystal changes under the action of electric fields. Optical electric field sensors have wide frequency bands and high sensitivity, and have been used in applications such as substations. However, the optical module is always large in size and high in cost, which cannot realize the large-scale arrangement of the sensor. The electric field sensor based on Micro-Electro-Mechanical System (MEMS) is another type of electric field sensor [15-18]. Under the action of electric fields, the conductor will produce induced charges. The induced charge is changed by the vibrating shielding electrode, thereby generating an induced current. This type of sensor can be prepared based on micro-fabrication process, so it is often small in size and low in cost. However, the vibrating electrode causes high power consumption and short life.

Piezoelectric materials deform under the action of electric fields, which is called the inverse piezoelectric effect. Due to the wide frequency bandwidth, high response amplitude and high temperature stability, piezoelectric materials are also used in the design of electric field sensors [19-24]. In this paper, a new type of micro electric field sensor is designed by combining piezoelectric film and piezoresistive film. At the same time, this article also carried out the parameter optimization and processing design of the sensor.

2 Structural design

The structure of the proposed micro electric field sensor is shown in Fig. 1. The structure of the sensor consists of a piezoelectric film, a silicon film and a cavity under the films. Four piezoresistive sensing elements are prepared onto the silicon film, which are formed by doping in the silicon film. The four sensing elements are connected by aluminum to form a Wheatstone bridge. We use P(VDF-*co*-TrFE) as the piezoelectric film. The piezoelectric film is coupled onto the silicon film. The thickness of the two layers of film is about tens of microns. The cavity can ensure the free vibration of the two films under the action of the electric field. The periphery of the silicon film is fixed on the silicon substrate,

and a silicon oxide insulating layer is arranged between the film and the substrate.

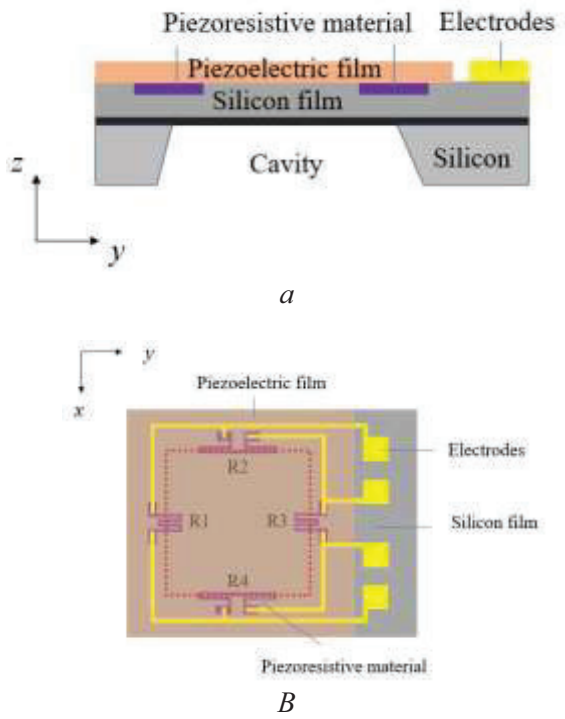

Fig. 1 Structure of the sensor. (a) A cross-section view of the sensor structure, (b) An overhead view of the sensor structure

Under the action of the electric field in the vertical direction, the piezoelectric film will stretch or shrink in the horizontal direction due to the piezoelectric coefficients d_{31} and d_{32}. Due to the surrounding fixation, the piezoelectric film will be convex or concave, thereby driving the silicon film to deform. The magnitude of the deformation of the piezoelectric material is characterized by the piezoelectric coefficient. A large piezoelectric coefficient will produce a large deformation. At the same time, the internal electric field of the dielectric material will be weakened under the space electric field. The larger the dielectric constant is, the smaller the internal electric field of the material will be. Therefore, the piezoelectric material needs to have a large piezoelectric coefficient and a small dielectric constant. Piezoelectric ceramics have a large piezoelectric coefficient, but often have a large dielectric constant. Organic piezoelectric materials have a small dielectric constant, but often have a small piezoelectric coefficient. P(VDF-*co*-TrFE) is an organic binary copolymer. It has both a small dielectric constant and a relatively large piezoelectric coefficient. So it is suitable for the proposed sensor.

The piezoresistive effect refers to the change in the resistivity of the semiconductor under the action of stress. Under the action of the piezoelectric film, the silicon film will deform up or down. In the area of the piezoresistive material, the internal strain of the silicon film will cause the resistance of the silicon to change. The piezoresistive materials are connected to form a Wheatstone bridge, and the four piezoresistive materials are respectively located on the four bridge arms. A voltage is applied across the Wheatstone bridge, and the voltage at the other ends of the Wheatstone bridge will change due to the change in resistance. By measuring the differential voltage generated by the Wheatstone bridge, the electric field can be measured.

We use finite element analysis to simulate the response of the sensor under an electric field of 10 kV/cm via Comsol Multiphysics, as shown in Fig. 2. Fig. 2 (a) and (b) respectively show the displacement response of the sensor when the electric field is applied along the *z*-axis direction and when applied along the opposite direction of the *z*-axis. It can be seen from the results that under the action of an electric field, the piezoelectric film will drive the silicon film to deform. At the center of the cavity, the membrane has the largest displacement. When the electric field is applied along the *z*-axis, the piezoelectric film stretches in the horizontal direction, driving the silicon film to sag downward. When the direction of the electric field is applied in the opposite direction of the *z*-axis, the piezoelectric film shrinks, driving the silicon film to bulge upward.

Fig. 2 (c) and (d) show the XX and YY components of the film strain when the electric field is applied along the *z*-axis. It can be seen from the figure that the largest strain on the film is at the edge of the cavity. Therefore, when the piezoresistive material is set, the doped region should be set at the edge of the cavity to obtain the maximum response of the sensor.

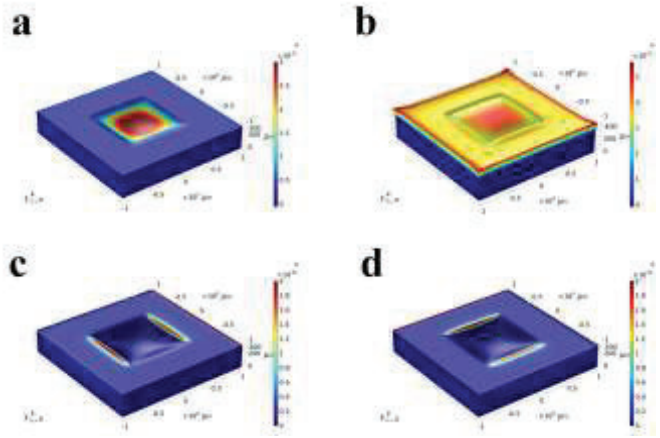

Fig. 2 Response of the sensor under electric fields. (a) Displacement distribution when the electric field is along the *z*-axis. (b) Displacement distribution when the electric field is in the opposite direction of the z-axis. (c) XX strain component distribution. (d) YY strain component distribution

When electric fields of different amplitudes are applied, the response of the electric field will change, as shown in Fig. 3. Fig. 3 (a) shows the strain distribution of the sensor under different electric fields. Fig. 3 (b) shows the maximum strain of the sensor under electric fields of different directions and different amplitudes. When the electric field amplitude increases, the strain of the sensor increases, and the maximum strain has a linear relationship with the electric field amplitude. At the same time, when the electric field is

applied along the *z*-axis, the response of the sensor is slightly greater than when the electric field is applied along the negative *z*-axis.

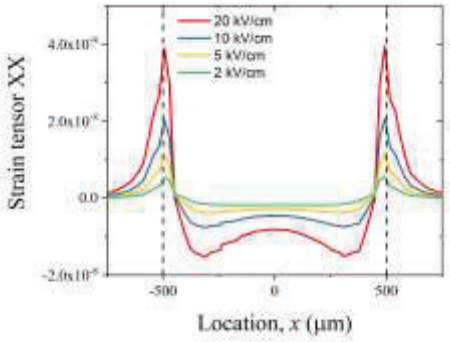

a

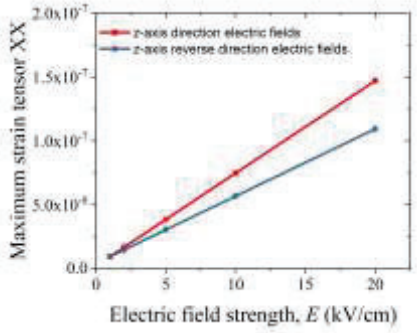

b

Fig. 3 Sensor response at different electric-field strengths. (a) XX strain component distribution curve of the silicon layer along the centre line. (b) The maximum XX strain component

In order to improve the response of the sensor, the sensor parameters need to be designed. The parameters affecting the proposed micro electric field sensor mainly include the side length of the cavity and the thickness of the piezoelectric film. This section studies the relationship between sensor response and parameters.

Fig. 4 (a) shows how the sensor strain distribution changes with the cavity size. When the size of the cavity increases, the deformation of the silicon film increases, and accordingly, the strain of the silicon film also increases. At the same time, as the size of the cavity increases, the maximum strain position of the sensor also changes. However, when the size of the cavity is too large, it may cause problems such as a decrease in the mechanical strength of the film. Therefore, the cavity size is generally selected below 1 mm.

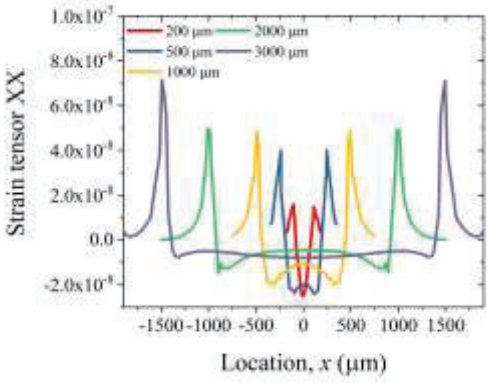

a

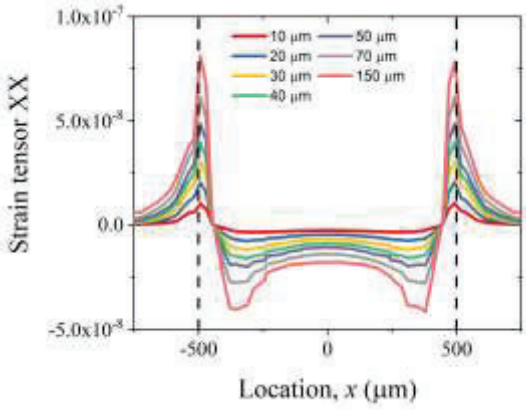

b

Fig. 4 (a) Relationship between distribution of strain and cavity side length. (b) Relationship between distribution of strain and piezoelectric film thickness.

When the thickness of the piezoelectric film increases, under the action of an electric field, the force generated by the piezoelectric material will increase, thereby increasing the deformation of the silicon film. Therefore, the strain of the film increases as the thickness of the piezoelectric film increases. When the thickness of the piezoelectric film changes, the sensor strain distribution remains unchanged. When the thickness of the piezoelectric film increases to a certain extent, the increase in film deformation mainly acts on the inside of the film and cannot be effectively transmitted to the silicon film. Therefore, the increase in strain of the silicon film will gradually become saturated. In the actual processing process, choose 50 μm as the piezoelectric film thickness.

In addition to cavity size and piezoelectric film thickness, there are other parameters that affect sensor response, such as silicon film thickness, piezoelectric film material, etc. However, due to the limitation of the processing technology, these parameters are specific values during the processing.

For the cavity size, the increase in the sensor cavity size will increase the displacement of the film on the one hand, and increase the initial value of the sensor capacitance on the other hand. Therefore, an increase in the cavity size will

greatly increase the resolution of the sensor. Within the size requirement, the larger the cavity size, the higher the sensor resolution.

3 Fabrication

The fabrication process of the proposed micro electric field sensor is based on a 4-inch SOI (Silicon-On-Insulator) wafer. A layer of 20 nm silicon oxide is grown on the SOI wafer as a protective layer for ion implantation. A certain dose and certain energy of boron ions are injected into the silicon wafer, forming the shape of the piezoresistive material. The wafer is annealed at a high temperature to activate the implanted ions. After removing the surface silicon oxide, a layer of 400 nm silicon oxide is grown onto the surface of the wafer. The silicon oxideof the wafer is etched by Inductively Coupled Plasma Etching (ICP Etching) to release the ohmic contact area on the surface of the wafer. After that, aluminum is vapor-deposited on the surface of the device layer, and the electrode shape is prepared by photolithography and wet etching. The P(VDF-co-TrFE) powder is mixed into a solution and spin-coated on the wafer surface. DMF is selected as the solvent. The concentration of the solution will affect the thickness of the P(VDF-co-TrFE) film. The solvent is evaporated in a vacuum oven and the piezoelectric material is polarized. The material is polarized under an electric field of 140 MV/m at 90 ℃. The piezoelectric film is patterned to expose the electrodes. The handle layer of the wafer is etched to release the thin film structure and form a cavity. Finally, the sensor is packaged and wired onto PCB board.

Use the electric field sensor test platform to test the sensor. The parallel plate electrodes are used to generate an electric field, and the output voltage of the sensor is measured by a differential amplifier and an oscilloscope. The resolution of the sensor can reach 200 V/m, and the measured electric field amplitude can reach 10 MV/m. At the same time, the size of the sensor is 4mm × 4mm, which has the characteristics of small size, low cost, and easy mass production. So it is suitable for the applications of large-scale sensor nodes

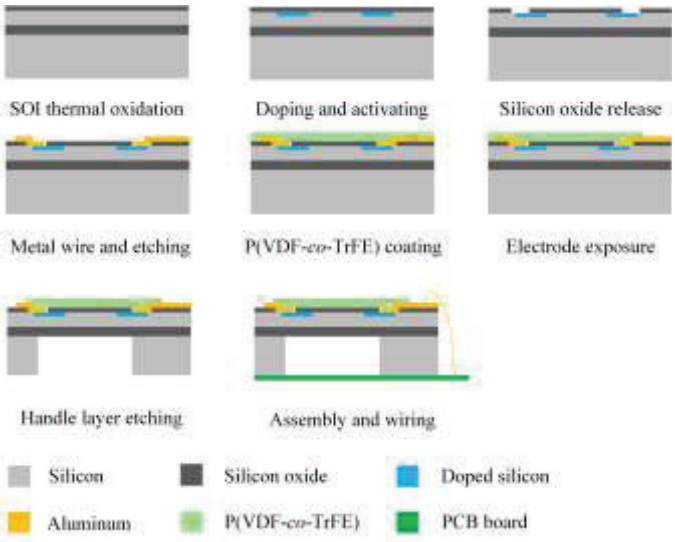

Fig. 5 Schematic illustration of the sensor fabrication.

4 Conclusion

We proposed a new structure of sensor using piezoelectric film. Through theoretical calculation and finite element simulation analysis, we verified the principle of the proposed sensor. We studied the influence of sensor parameters on sensor performance, and optimized the sensor performance. Finally, we designed a sensor processing program based on the micro-fabrication technology to realize the mass production of the sensor, which lays a foundation for the application of the micro electric field sensor in the Ubiquitous Power Internet of Things.

5 Acknowledgements

This work was supported in part by the Guizhou Province Smart Sensing and Transparent Grid Technology Innovation Talent Technical Team under Talents of Qiankehe Platform 【2020】5015.

6 References

[1] Gubbi, J., Buyya, R., Marusic, S., and Palaniswami, M., 'Internet of Things (Iot): A Vision, Architectural Elements, and Future Directions', Future generation computer systems, 2013, 29, (7), pp. 1645-1660.

[2] Huang, A.Q., Crow, M.L., Heydt, G.T., Zheng, J.P., and Dale, S.J., 'The Future Renewable Electric Energy Delivery and Management (Freedm) System: The Energy Internet', Proceedings of the IEEE, 2010, 99, (1), pp. 133-148.

[3] Si, D., Wang, J., Wei, G., and Yan, X., 'Method and Experimental Study of Voltage Measurement Based on Electric Field Integral with Gauss–Legendre Algorithm', IEEE Transactions on Instrumentation and Measurement, 2019, 69, (6), pp. 2771-2778.

[4] Zhang, B., Hao, Z., and Bo, Z., 'Development of Relay Protection for Smart Grid (1): New Principle of Fault Distinction', Electric Power Automation Equipment, 2010, 30, (1), pp. 1-6.

[5] Duan, L., Hu, J., Zhao, G., Chen, K., Wang, S.X., and He, J., 'Method of Inter-Turn Fault Detection for Next-Generation Smart Transformers Based on Deep Learning Algorithm', High Voltage, 2019, 4, (4), pp. 282-291.

[6] Jiang, H., Zhang, J.J., Gao, W., and Wu, Z., 'Fault Detection, Identification, and Location in Smart Grid Based on Data-Driven Computational Methods', IEEE Transactions on Smart Grid, 2014, 5, (6), pp. 2947-2956.

[7] Chen, W., Wang, J., Wan, F., and Wang, P., 'Review of Optical Fibre Sensors for Electrical Equipment Characteristic State Parameters Detection', High Voltage, 2019, 4, (4), pp. 271-281.

[8] Zeng, S., Powers, J.R., and Newbraugh, B.H., 'Effectiveness of a Worker-Worn Electric-Field Sensor to

Detect Power-Line Proximity and Electrical-Contact', Journal of safety research, 2010, 41, (3), pp. 229-239.
[9] Han, Z., Xue, F., Hu, J., and He, J., 'Micro Electric-Field Sensors: Principles and Applications', IEEE Industrial Electronics Magazine, 2021.
[10] Yang, P., Chen, B., Wen, X., Peng, C., Xia, S., and Hao, Y., 'A Novel Mems Chip-Based Atmospheric Electric Field Sensor for Lightning Hazard Warning Applications', in, 2015 IEEE SENSORS, (IEEE, 2015)
[11] Zeng, R., Wang, B., Yu, Z., and Chen, W., 'Design and Application of an Integrated Electro-Optic Sensor for Intensive Electric Field Measurement', IEEE Transactions on Dielectrics and Electrical Insulation, 2011, 18, (1), pp. 312-319.
[12] Zeng, R., Yu, J., Wang, B., Niu, B., and Hua, Y., 'Study of an Integrated Optical Sensor with Mono-Shielding Electrode for Intense Transient E-Field Measurement', Measurement, 2014, 50, pp. 356-362.
[13] Tajima, K., Kobayashi, R., KUWABARA, N., and TOKUDA, M., 'Development of Optical Isotropic E-Field Sensor Operating More Than 10 Ghz Using Mach-Zehnder Interferometers', IEICE transactions on electronics, 2002, 85, (4), pp. 961-968.
[14] Schwerdt, M., Berger, J., Schuppert, B., and Petermann, K., 'Integrated Optical E-Field Sensors with a Balanced Detection Scheme', IEEE transactions on electromagnetic compatibility, 1997, 39, (4), pp. 386-390.
[15] Riehl, P.S., Scott, K.L., Muller, R.S., Howe, R.T., and Yasaitis, J.A., 'Electrostatic Charge and Field Sensors Based on Micromechanical Resonators', Journal of Microelectromechanical Systems, 2003, 12, (5), pp. 577-589.
[16] Peng, C., Yang, P., Zhang, H., Guo, X., and Xia, S., 'Design of a Novel Closed-Loop Soi Mems Resonant Electrostatic Field Sensor', Procedia Engineering, 2010, 5, pp. 1482-1485.
[17] Ma, Q., Huang, K., Yu, Z., and Wang, Z., 'A Mems-Based Electric Field Sensor for Measurement of High-Voltage Dc Synthetic Fields in Air', IEEE Sensors Journal, 2017, 17, (23), pp. 7866-7876.
[18] Kainz, A., Steiner, H., Schalko, J., Jachimowicz, A., Kohl, F., Stifter, M., Beigelbeck, R., Keplinger, F., and Hortschitz, W., 'Distortion-Free Measurement of Electric Field Strength with a Mems Sensor', Nature electronics, 2018, 1, (1), pp. 68-73.
[19] Xue, F., Hu, J., Guo, Y., Han, G., Ouyang, Y., Wang, S.X., and He, J., 'Piezoelectric–Piezoresistive Coupling Mems Sensors for Measurement of Electric Fields of Broad Bandwidth and Large Dynamic Range', IEEE Transactions on Industrial Electronics, 2019, 67, (1), pp. 551-559.
[20] Xue, F., Hu, J., Wang, S.X., and He, J., 'Electric Field Sensor Based on Piezoelectric Bending Effect for Wide Range Measurement', IEEE Transactions on Industrial Electronics, 2015, 62, (9), pp. 5730-5737.
[21] Han, Z., Xue, F., Yang, J., Hu, J., and He, J., 'Micro Piezoelectric-Capacitive Sensors for Highsensitivity Measurement of Space Electric Fields', in, 2019 IEEE SENSORS, (IEEE, 2019)
[22] Han, Z., Xue, F., Yang, G., Yu, Z., Hu, J., and He, J., 'Micro-Cantilever Capacitive Sensor for High-Resolution Measurement of Electric Fields', IEEE Sensors Journal, 2020.
[23] Xue, F., Hu, J., Wang, S.X., and He, J., 'Optimum Direct Current Magnetic Bias in Ferromagnetic Phase for Improvement of Magnetoelectric Effect', Applied Physics Letters, 2015, 106, (26), p. 262902.
[24] Xue, F., Hu, J., Wang, S.X., and He, J., 'In-Plane Longitudinal Converse Magnetoelectric Effect in Laminated Composites: Aiming at Sensing Wide Range Electric Field', Applied Physics Letters, 2015, 106, (8), p. 082901.